Proc. of the European Safety and Reliability Conference (ESREL 2026)
Edited by José C. Matos, Paulo B. Lourenço, Michael Beer, Daniel Oliveira, Edoardo Patelli, Hélder S. Sousa, Rui A. Silva and Monica Santamaria

Published by Research Publishing, Singapore.
doi: 10.3850/ESREL2026061419_esrel26-p27620-cd

Development of a Novel Replaceable Steel Fuse for Earthquake-Resilient Precast Concrete Frames

Ali Ghamari

Department of Civil Engineering, Il.C., Islamic Azad University, Ilam, Iran. ali.ghamari@iau.ac.ir

Imran Karimi

Department of Civil Engineering, University of Tabriz, Tabriz, Iran. E-mail: imrankarimi1992@gmail.com

Shaghayegh Karimzadeh

University of Minho, ISISE, ARISE, Department of Civil Engineering, Guimarães, Portugal. E-mail: shaghkn@civil.uminho.pt

Paulo B. Lourenço

University of Minho, ISISE, ARISE, Department of Civil Engineering, Guimarães, Portugal. E-mail: pbl@civil.uminho.pt

Abstract: Precast concrete frames offer advantages in rapid construction, high-quality industrial production of structural elements, and cost-effectiveness. However, past earthquakes have demonstrated their vulnerability to seismic damage. Although various mitigation methods have been proposed, most are complex to fabricate or fail to meet economic requirements. To address this limitation, the present paper introduces an innovative system integrating replaceable steel links with precast concrete frames, evaluated through parametric and numerical studies. The steel links are simple to fabricate, install, and replace following a major earthquake. Results show that yielding is confined to the steel links, allowing the concrete components to remain elastic. The links thus function as ductile fuses, effectively dissipating seismic energy. Comparing the results indicated that link with shear mechanism has a better performance than links with shear-flexural or flexural mechanism while the ratio of plastic moment of link capacity to the concrete beam remain less than one.

Keywords: Precast concrete frames; Replaceable steel links; Ductile fuses; Seismic energy dissipation; Shear mechanism.

1. Introduction

The seismic performance of precast concrete frames (PCF), including moment-resisting systems and gravity-load frames with precast beams, columns, and connections (dry, wet, or hybrid), has been extensively documented through post-earthquake reconnaissance and research. Precast construction offers advantages in speed, quality control, and cost, but earthquakes have repeatedly revealed vulnerabilities associated with inadequate connection detailing, insufficient ductility and moment transfer capacity, short bearing lengths, lack of confinement, and weak integration with the lateral force-resisting system. Such deficiencies can promote brittle connection failures, compromise gravity-load continuity (e.g., loss of seating), and increase residual drifts; in severe cases, they may contribute to disproportionate/progressive collapse, whereas well-detailed cast-in-place moment frames are intended to develop more ductile, distributed plastic hinging (Dal Lago et al. 2019; Guerrero et al. 2019).

Post-event studies repeatedly document that precast frames and single-storey precast industrial buildings can perform poorly when seismic provisions are limited or are not effectively implemented, with damage frequently concentrated in diaphragms and connections rather than in ductile frame mechanisms. In the 1994 Northridge earthquake (USA), many engineered precast buildings performed well; however, several precast parking structures experienced severe damage and collapses, with prominent problems in diaphragm/collector load paths and unintended participation of gravity columns due to inadequate ties and detailing (Iverson and Hawkins 1994). The 2012 Emilia earthquakes (Italy) again highlighted the vulnerability of common single-storey precast systems, where failures of beam-to-column and roof-element connections led to loss of support and multiple collapses, including buildings designed to then-current practice (Belleri et al. 2014; Magliulo et al. 2014; Dal Lago et al. 2017). Overall, observed failures are commonly linked to connection deficiencies and limited ductility, often exacerbated by P-Δ demands, diaphragm/collector weaknesses, and adverse infill interactions.

Recent events underscore ongoing vulnerabilities in precast industrial and single-storey systems when connection detailing and robustness are inadequate. Following the 6 February 2023 Kahramanmaraş earthquakes (Türkiye–Syria; M_w 7.8 and 7.5), field observations and subsequent studies reported frequent damage concentrated at precast connections and support regions, including beam–column connection distress, loss of seating/support of roof elements, and collapse mechanisms associated with insufficient anchorage/ties and limited ductility (Arslan et al. 2024). In contrast, reconnaissance reports for the 3 April 2024 Hualien earthquake (Taiwan; M_w ~7.2–7.4) describe comparatively limited structural impacts overall, consistent with strengthened seismic design and retrofit practice developed after major past events such as 1999 Chi-Chi; no widespread precast industrial collapses are highlighted in the main summaries (NCREE/EERI recon).

Predominant damage modes include: (a) connection failures (brittle shear/tension, dowel pull-out, inadequate grouting/anchorage) which can lead to loss of support and, in severe cases, disproportionate/progressive collapse (e.g., industrial precast collapses in Emilia 2012 and connection-related failures reported after the 2023 Kahramanmaraş earthquakes); (b) joint cracking/spalling associated with inadequate force transfer or missing shear keys; (c) column vulnerabilities (short-column shear due to infills, confinement-related buckling, and P-Δ instability; (d) bearing/support loss; (e) diaphragm/floor damage (including hollow-core unit cracking at relatively low drift demands); (f) non-ductile global behaviour with limited and poorly distributed energy dissipation. Non-emulative precast systems tend to concentrate damage at joints and interfaces, whereas well-detailed cast-in-place moment frames are intended to develop more distributed ductile hinging.

Reconnaissance across multiple earthquakes and coordinated research programmes have motivated stronger, more robust precast connections and low-damage concepts, including emulative connections, supplemental dissipaters, self-centring/post-tensioned rocking, and replaceable "fuse" elements (Priestley et al. 2003; Fleischman et al. 2014). Traditional precast moment frames can suffer brittle joint behaviour, damage concentration at interfaces, and challenging post-earthquake repair. Replaceable steel fuses (e.g., angles, plates, miniature buckling-restrained brace (BRB)-type elements) address this by localising inelastic deformation and energy dissipation in sacrificial components, protecting precast members and enabling rapid bolted replacement (Pratap et al. 2023). The fuse concept originated in steel systems (e.g., replaceable links in braced frames) and was later adapted to concrete through post-tensioned rocking/self-centring frameworks; applications in precast systems expanded markedly during the 2010s–2020s in pursuit of accelerated construction and improved resilience (Saravanan et al. 2018; Pratap et al. 2023). Reviews covering 2000–2022 show an early emphasis on steel "small replaceable component" strategies followed by broader uptake in hybrid and concrete-based low-damage solutions (Pratap et al. 2023).

Recent examples include precast moment connections using top shear tabs for shear transfer and bottom replaceable BRB fuses for energy dissipation, with gaps that permit controlled rotation and aim to confine damage primarily to the fuses (Yang et al. 2025). Bio-inspired replaceable hinge connections (RBHCs) have also been proposed for reinforced-concrete (RC) frame beam ends and column bases using thin steel plates to enhance damage control and ductility (An et al. 2025). Other related replaceable/low-damage devices include staged-yield connections and detachable steel-plate mechanisms, as well as external angle/steel energy-dissipation details reported in the precast/self-centring literature (Huang et al. 2022; Ro et al. 2024). Experimental studies commonly report stable hysteresis with damage concentrated in replaceable elements, improved repairability, and reduced downtime; some systems explicitly target immediate-occupancy-level performance for moderate shaking (Pratap et al. 2023). Overall, replaceable steel fuse concepts offer a practical pathway to low-damage, repairable precast frames, supporting rapid post-earthquake recovery and reduced life-cycle impacts.

2. Proposed System

Precast concrete frames can achieve satisfactory seismic performance when connections are properly detailed, and the system is well integrated within the lateral force-resisting mechanism. Nevertheless, earthquake observations have repeatedly shown that deficiencies in connection behaviour and limited ductility can concentrate damage, increase residual deformations, and make post-event repair costly and complex. These lessons motivate the development of low-damage, repairable precast solutions for seismic regions. Accordingly, this study proposes a novel ductile, replaceable steel link that incorporates a steel connection component, as illustrated in Figure 1.

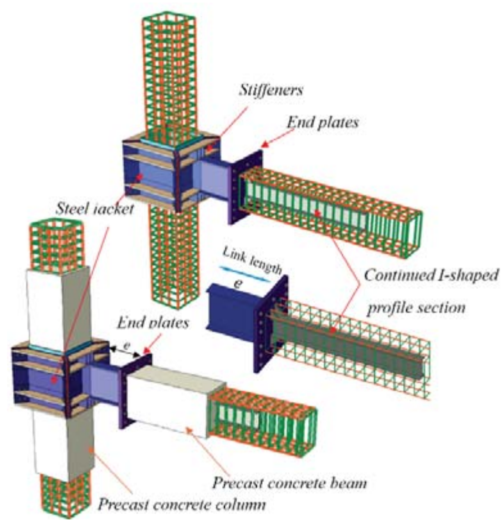

Fig. 1. The proposed system.

The steel link is intentionally designed to yield under lateral seismic loading so that, after strong shaking, damage is primarily confined to this sacrificial component and can be addressed through simple, low-cost replacement. By promoting plastic hinge formation within the I-shaped steel link, the system is intended to provide stable hysteretic response and enhanced energy dissipation, while limiting damage to the surrounding precast members and connections.

3. Parametric Study

To evaluate the proposed system, two analysis series are performed. In the first series, detailed finite-element (FE) models are developed in ABAQUS to capture component interaction and local response. The concrete components are kept identical, while the steel link properties and geometry are varied to identify the optimal link configuration for the preliminary design.

In the second series, the structural performance of two representative multi-storey RC frames is assessed by comparing (i) a conventional cast-in-place RC moment frame and (ii) a precast concrete frame incorporating the proposed ductile fuse with the optimal link configuration obtained from Series 1. The boundary conditions for Series 1 are shown in Figure 2, and the plan and schematic views of the frames analysed in Series 2 are provided in Figure 3. The case-study buildings are 3- and 4-storey frames with a 3-bay layout in each principal direction (3×3 bays). The bay spacing is 7 m, and the storey height is 3.2m (constant over all storeys), as shown in Figure 3

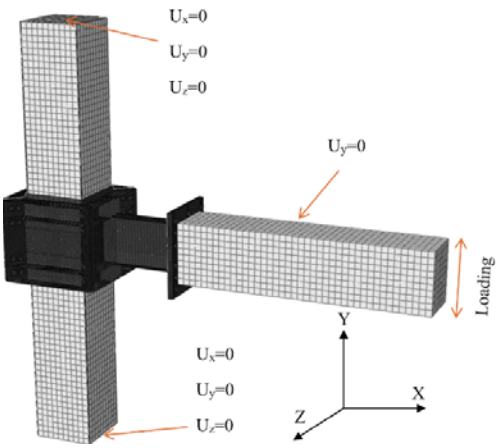

Fig. 2. Boundary conditions.

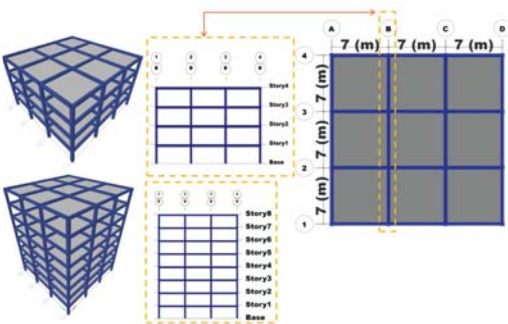

Fig. 3. The properties of the multi-story RC structures.

To develop the first-series models, an I-shaped steel link was initially designed to have a flexural capacity comparable to that of the RC beam. The baseline link had a length e = 500 mm, web thickness t_w = 8 mm and web height h_w = 400 mm, and flange width b_f = 140 mm with flange thickness t_f = 10 mm. A strength ratio was then defined as $\Psi = M_{ub} / M_p$, where M_p is the plastic moment capacity of the steel link and M_{ub} is the flexural capacity of the RC beam. To vary Ψ, the flange thickness was adjusted to t_f = 15, 10, 5, and 2.5 mm, yielding Ψ = 1.34, 1.00, 0.68, and 0.52, respectively.

Following AISC 341-22, the dominant link mechanism is characterised using $\rho = (eV_p)/M_p$, where V_p is the plastic shear capacity of the link. Links are classified as shear-dominated for $\rho \leq 1.6$ (very short: $\rho \leq 1.0$; short: $1.0 < \rho \leq 1.6$), shear–flexure (medium) for $1.6 < \rho \leq 2.6$, and flexure-dominated (long) for $\rho > 2.6$. Based on this definition, the analysed links result in ρ = 0.81, 1.07, 1.59, and 2.08, respectively.

Additionally, for the second analysis series, 4- and 8-storey structures were designed in accordance with ASCE 7-22 and ACI 318-22. The same architectural plan and bay layout were adopted for both buildings. Figure 3 presents the models considered in the second series.

4. *Numerical Study*

4.1. Numerical Models

The FE models introduced in the parametric study were analysed in ABAQUS. After defining the geometry and material properties, each component was meshed using an appropriate discretisation scheme. Model parts were meshed separately and then assembled using the specified interaction/contact definitions. Concrete components, bolts, and end plates were modelled with three-dimensional solid elements. Reinforcing bars were represented using embedded wire (truss/beam) elements, while the I-shaped steel link (web and flanges) was modelled using shell elements to capture local buckling and yielding behaviour efficiently.

4.2. Materials and boundary conditions

For both analysis series, the concrete compressive strength was taken as f'_c = 30 MPa and the reinforcing steel yield strength as f_y = 400 MPa. All steel components (link, plates, and related connection parts) were modelled using S235 steel in accordance with EN 10025-2 (grade S235JR). The boundary conditions shown in Figure 3 were applied. Cyclic displacement-controlled loading, following the ATC-24 protocol, was imposed at the free end of the beam. At the mid-height of the columns, where the bending moment is assumed to be zero, rotational degrees of freedom were released while translational degrees of freedom were constrained according to the symmetry condition. In addition, to represent diaphragm restraint from the floor system, the out-of-plane displacement of the beam was restrained (U_z = 0).

4.3. Verification of FE results

To assess the accuracy of the FE modelling approach, the experimental study by Chen et al. (2022) on a hybrid RC frame with steel connection details was selected as a benchmark. In that test programme, steel connection components were used to form moment-resisting joints between precast concrete elements. Figure 4 compares the FE predictions with the experimental response. Overall, the numerical results show good agreement with the test data. In particular, the initial elastic stiffness is well captured, and the model reproduces the nonlinear response with a small deviation from the experimental curve.

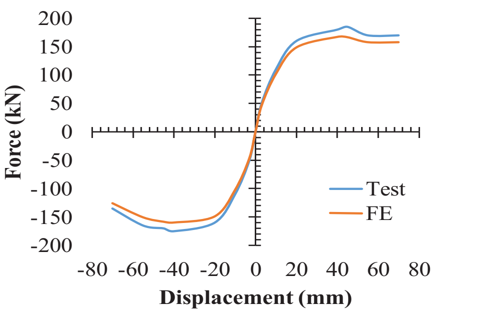

Fig. 4. Comparing the FE and experimental test results (Chen 2022).

5. Discussion and Results

5.1. Overall yielding state

Figure 5 illustrates the yielding states of the analysed models. As expected, plastic hinging is concentrated in the steel link. The results indicate that increasing Ψ increases the stress demand transferred through the end plate, which may drive the adjacent concrete components into nonlinear response. Accordingly, maintaining $\Psi \leq 1$ is expected to keep the concrete components predominantly elastic and to confine inelasticity to the replaceable link. Figure 5 also shows that when the flange thickness is approximately 5 mm, local buckling develops concurrently with yielding. This instability is reflected in the hysteresis response as strength/stiffness degradation, discussed in the following sections. Therefore, satisfying compactness (seismically compact section requirements) in accordance with AISC 360-22 is necessary to delay local buckling and ensure stable cyclic behaviour.

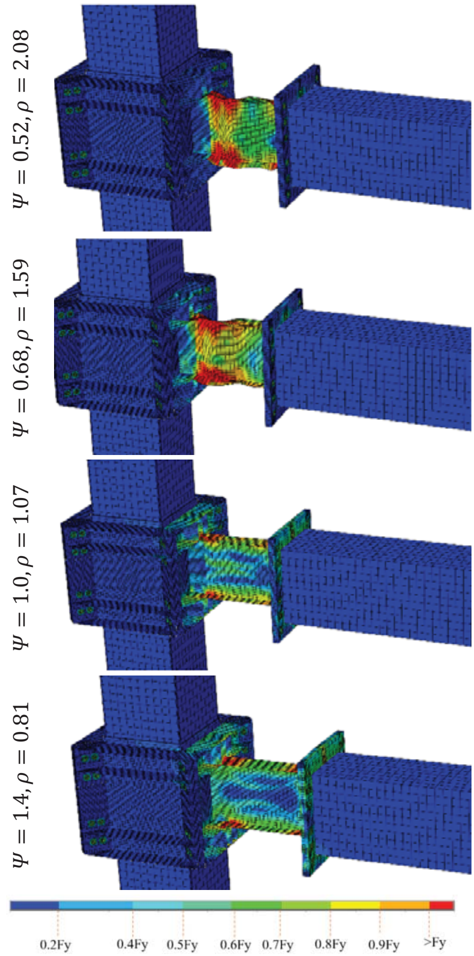

Fig. 5. Yielding statues of the models.

5.2. Hysteresis curves

Figure 6 compares the hysteresis responses of the FE models. The cyclic behaviour is governed by the link mechanism and is primarily influenced by (i) the link classification parameter ρ, (ii) the strength ratio Ψ, and flange slenderness (which affects local buckling). For shear-dominated links ($\rho \leq 1.6$), the response exhibits relatively stable hysteresis loops with limited pinching and gradual degradation. As Ψ approaches or exceeds 1.0, the curves become more similar because part of the lateral resistance is no longer provided solely by the steel link; the surrounding RC components and reinforcement increasingly participate in resisting the imposed actions. This increased participation is also consistent with the sudden strength/rotation drop observed around a drift demand of approximately 0.03 rad, indicating a change in the dominant inelastic mechanism and/or the onset of local instability/damage outside the intended fuse region. Accordingly, a target range of $0.9 \leq \Psi \leq 1.0$ is recommended to confine inelastic demand primarily to the steel link while limiting unintended nonlinear response in the surrounding concrete components. The $0.9 \leq \Psi$ is selected to satisfy the economical aspect.

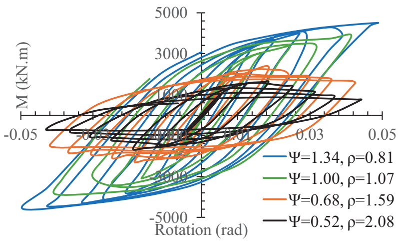

Fig. 6. Comparing the hysteresis curves.

5.3. *Ultimate strength and stiffness*

Table 1 summarises the ultimate flexural capacity, M, and initial stiffness, K, obtained from the FE models. For comparison, all results are normalised by the corresponding values of the reference model with $\Psi = 1.0$. The results indicate that variations in the steel link have a stronger influence on ultimate flexural capacity than on stiffness. Across the analysed range, the ultimate bending capacity scales approximately with Ψ (about 1.2Ψ relative to the reference); however, this trend should be confirmed through a broader parametric set and additional validation.

Table 1. Ultimate strength and stiffness.

Ψ	ρ	K (N/mm)	M (kN.m)	$\frac{\text{Model } i}{\text{Model } \Psi = 1}$ K	M
1.34	0.81	3434.34	4513.09	1.15	1.17
1.00	1.07	2987.95	3866.26	1.00	1.00
0.68	1.59	2572.33	2281.86	0.86	0.59
0.52	2.08	2107.28	1613.90	0.71	0.42

5.4. *Energy dissipation*

Figure 7 presents the energy dissipation of the analysed models. Up to a link rotation of about 0.02 rad, the specimens with shear- and shear–flexure-dominated mechanisms exhibit similar cumulative energy dissipation. Models with shear links ($\rho \leq 1.6$) generally provide higher energy dissipation than the other configurations; however, for cases with $\Psi < 1$ ($\Psi = 0.68$, $\Psi = 0.52$), a noticeable degradation appears at link rotations of approximately 0.03 rad. This reduction becomes more pronounced as cumulative plastic deformation increases, indicating reduced stability of the hysteretic response under large cyclic demands. These results confirm that, to achieve desirable performance, the link should be designed within $0.9 \leq \Psi \leq 1.0$, consistent with the findings in Section 5.2.

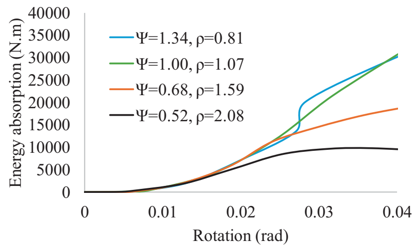

Fig. 7. Comparing the energy absorption of the FE models.

5.3. *Comparing the RC and the precast RC equipped with steel links*

In the analysed buildings, beams govern the reinforcement demand and typically require substantially higher longitudinal reinforcement than other members. Because the proposed precast frames and the conventional cast-in-place RC frames share the same slabs and columns, the comparison is focused on the required beam flexural reinforcement (Figures 8 and 9). All reinforcement quantities were designed in accordance with ACI provisions.

The results show that introducing the ductile steel link reduces the required beam flexural reinforcement by approximately 1.2–1.67 times for the 4-storey building and by about 1.2 to more than 2.0 times for the 8-storey building. These reductions indicate a potential economic benefit of the proposed approach through lower reinforcement demand (and associated fabrication/placement), although overall cost-effectiveness should also account for the steel link and connection hardware.

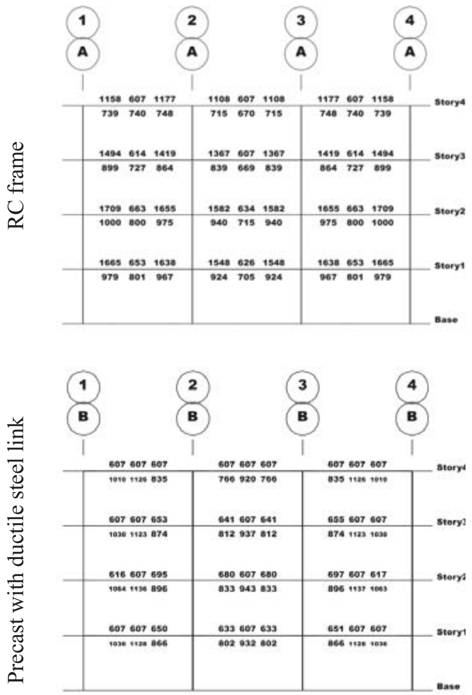

Fig. 8. The required flexural reinforcements of the concert beams for 4-storey structures.

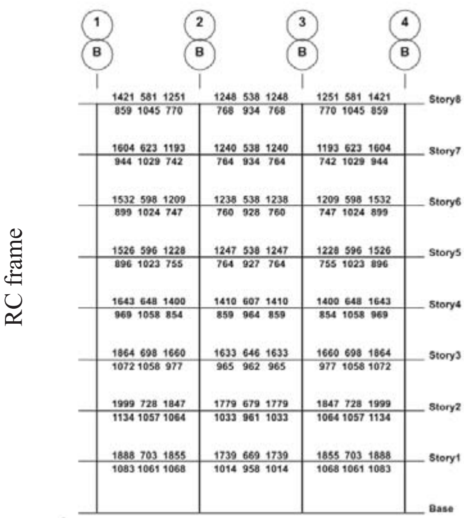

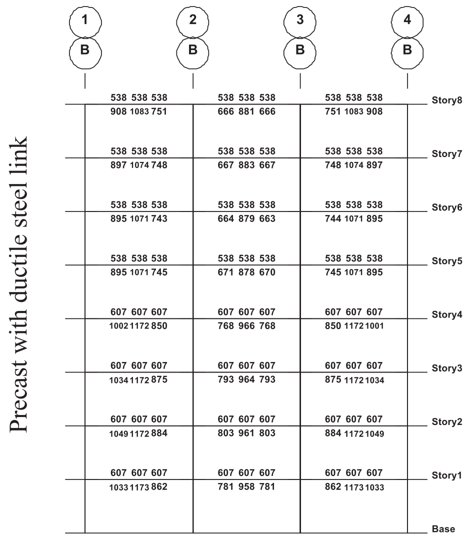

Fig. 9. The required flexural reinforcements of the concert beams for 8-storey structures.

6. Conclusions

In this paper, an innovative replaceable steel link to improve the seismic behaviour of precast concrete frames was proposed and investigated through numerical (FE) analyses and a parametric study. The main findings are summarised as follows:

- The proposed precast frame with the replaceable steel link concentrates inelastic demand in the steel fuse. For designs with $\Psi \leq 1$, the surrounding concrete components are expected to remain predominantly elastic over the analysed rotation range, supporting a repairable, low-damage response.
- The hysteretic response is governed by the link mechanism and key geometric parameters (e.g., link length/classification ρ, strength ratio Ψ, and flange slenderness). Shear-dominated links ($\rho \leq 1.6$) generally exhibit stable hysteresis loops, whereas increased flange slenderness promotes local buckling and earlier strength/stiffness degradation. To confine inelasticity to the link while limiting unintended demand on the concrete components, a design target of $0.9 \leq \Psi \leq 1.0$ is recommended.

- Plastic hinges formed in the steel link as intended. For thinner flanges (≈ 5 mm), local buckling developed concurrently with yielding, which was reflected in the hysteresis response as increased degradation. Therefore, satisfying seismically compact/compactness requirements in accordance with AISC 360-22 is important to delay local buckling and maintain stable cyclic behaviour.
- Cumulative energy absorption was similar among configurations up to approximately 0.02 rad. At larger rotations, shear-dominated links accumulated higher energy than the medium-link configuration; around ~0.03 rad, some cases showed a change in the rate of energy accumulation, consistent with the onset of additional mechanisms/instabilities observed in the hysteresis response.

Acknowledgments

This work was funded by the Fundação para a Ciência e a Tecnologia (FCT), I.P., through the R&D project "An innovative metallic damper for enhancing the seismic performance of reinforced concrete frames" with reference 2024.16312.PEX (https://doi.org/10.54499/2024.16312.PEX). This work was also supported by FCT/MCTES under the R&D Unit Institute for Sustainability and Innovation in Structural Engineering (ISISE), under the references UID/4029/2025 (https://doi.org/10.54499/UID/04029/2025) and UID/PRR/04029/2025 (https://doi.org/10.54499/UID/PRR/04029/2025), and under the Associate Laboratory Advanced Production and Intelligent Systems ARISE under reference LA/P/0112/2020 (https://doi.org/10.54499/LA/P/0112/2020).

References

An, A.-H., Wang W.-D., Yuan Y.-J., and Shi Y.-L. (2025). Seismic Performance of Precast Concrete Frame with Replaceable Bio-Inspired Hinge Connections. *Journal of Constructional Steel Research 235,* 109786. https://doi.org/10.1016/j.jcsr.2025.109786.

ACI-440-22, American Concrete Institute (2022). *Building Code Requirements for Structural Concrete Reinforced with Glass Fiber-Reinforced Polymer (GFRP) Bars—Code and Commentary*. Farmington Hills, MI: American Concrete Institute.

ANSI/AISC 341-22, American Institute of Steel Construction (2022). *Seismic Provisions for Structural Steel Buildings*. Chicago: American Institute of Steel Construction.

ASCE/SEI 7-22, American Society of Civil Engineers (2022). *Minimum Design Loads and Associated Criteria for Buildings and Other Structures*. Reston, VA: American Society of Civil Engineers.

Arslan, M. H., Y. Dere, A. S. Ecemiş, G. Doğan, M. Özturk, and S. Z. Korkmaz (2024). Code-Based Damage Assessment of Existing Precast Industrial Structures after the 2023 Kahramanmaraş Earthquakes. *Journal of Building Engineering 86*, 108811. ttps://doi.org/10.1016/j.jobe.2024.108811.

Belleri, A., E. Brunesi R. Nascimbene, M. Pagani, and P. Riva. (2014). Seismic Performance of Precast Industrial Facilities Following Major Earthquakes in the Italian Territory. *Journal of Performance of Constructed Facilities 29 (5)*, 04014135. https://doi.org/10.1061/(ASCE)CF.1943-5509.0000617.

Cavaco, E. S., J. R. Casas, L. A. C. Neves, and A. E. Huespe (2013). Robustness of Corroded Reinforced Concrete Structures: A Structural Performance Approach. *Structure and Infrastructure Engineering 9 (1)*, 42–58. https://doi.org/10.1080/15732479.2010.515597.

Chen, W., Y. Xie, X. Guo, D. Li (2022). Experimental Investigation of Seismic Performance of a Hybrid Beam–Column Connection in a Precast Concrete Frame. *Buildings 12*, 801. https://doi.org/10.3390/buildings12060801

Dal Lago, B., M. Ercolino, G. Magliulo, and G. Manfredi (2017). Empirical Seismic Fragility for the Precast RC Industrial Buildings Damaged by the 2012 Emilia (Italy) Earthquakes. *Earthquake Engineering & Structural Dynamics 46 (14)*, 2317–2335. https://doi.org/10.1002/eqe.2906.

Dal Lago, B., S. Bianchi, F. Biondini, and G. Toniolo. (2019). Diaphragm Effectiveness of Precast Concrete Structures with Cladding Panels under Seismic Action. *Bulletin of Earthquake Engineering 17*, 473–495. https://doi.org/10.1007/s10518-018-0452-3.

Ding, K., Y. Ye, and W. Ma (2021). Seismic Performance of Precast Concrete Beam-Column Joint Based on the Bolt Connection. *Engineering Structures 232*, 111884. https://doi.org/10.1016/j.engstruct.2021.111884.

EN 10025, *European Committee for Standardization. Hot Rolled Products of Structural Steels — Part 2: Technical Delivery Conditions for Non-Alloy Structural Steels*. EN 10025-2:2019. Brussels: CEN, 2019.

Fleischman, R. B., J. I. Restrepo, J. Maffei, K. Seeber, S. Pampanin, and F. Zahn (2014). Damage Evaluations of Precast Concrete Structures in the 2010–2011 Canterbury Earthquake Sequence. *Earthquake Spectra 30 (1)*, 277–306. https://doi.org/10.1193/031213eqs068m.

Guerrero, H., V. Rodriguez, J. A. Escobar, S. M. Alcocer, F. Bennetts, M. Suarez (2019). Experimental Tests of Precast Reinforced Concrete Beam-Column Connections. *Soil Dynamics and Earthquake Engineering 125*, 105743. https://doi.org/10.1016/j.soildyn.2019.105743.

Iverson, J. K., and N. M. Hawkins (1994). Performance of Precast/Prestressed Concrete Building Structures during Northridge Earthquake. *PCI Journal 39 (2)*, 38–55. https://doi.org/10.15554/pcij.03011994.38.55.

Ro, K. M., M. S. Kim, and Y. H. Lee (2024). An Experimental Study on the Seismic Performance of a Replaceable Steel Link System Acting as a Structural Fuse. *Applied Sciences 14 (6)*, 2358. https://doi.org/10.3390/app14062358.

Huang, H., M. Li, Y. Yuan, and H. Bai (2022). Experimental Research on the Seismic Performance of Precast Concrete Frame with Replaceable Artificial Controllable Plastic Hinges. *Journal of Structural Engineering 149 (1)*, 04022222. https://doi.org/10.1061/JSENDH.STENG-11648.

Magliulo, G., M. Ercolino, C. Petrone, O. Coppola, and G. Manfredi (2014). The Emilia Earthquake: Seismic Performance of Precast Reinforced Concrete Buildings. *Earthquake Spectra 30 (2)*, 891–912. https://doi.org/10.1193/091012EQS285M.

Pratap, M., and G. R. Vesmawala (2023). The State-of-the-Art Review on Development of Replaceable Fuse Components in Resilient Moment Resisting Frame. *Structures 56*, 104888. https://doi.org/10.1016/j.istruc.2023.104888.

Priestley, M. J. N. (2003). Myths and Fallacies in Earthquake Engineering, Revisited. Pavia: IUSS Press. (Seminal reference from PRESSS program influences; for full program, see also PRESSS reports such as Stanton and Nakaki 2002 on design guidelines for precast seismic systems.)

Saravanan, M., R. Goswami, and G. S. Palani (2018). Replaceable Fuses in Earthquake Resistant Steel Structures: A Review. *International Journal of Steel Structures 18 (3)*, 868–879. https://doi.org/10.1007/s13296-018-0035-9.

Sezen, H., A. S. Whittaker, K. J. Elwood, and K. M. Mosalam (2003). Performance of Reinforced Concrete Buildings during the August 17, 1999 Kocaeli, Turkey Earthquake, and Seismic Design and Construction Practise in Turkey. *Engineering Structures 25 (1)*, 103–114. https://doi.org/10.1016/S0141-0296(02)00121-9.

Yang, Z., J. Zhao, X. Yao, K. Jiang, W. Chen, and W. Han (2025). Precast Concrete Moment Connection with Top Shear Tabs and Bottom Replaceable BRB Fuses to Coordinate Structural Serviceability and Resilience. *Engineering Structures 340*, 120732. https://doi.org/10.1016/j.engstruct.2025.120732.